MODIFICATION OF THE TRANSVERSE ELECTRON BUNCH PROFILE WITH SPATIAL LIGHT MODULATOR AT FLUTE

T. Schmelzer*, M. Brosi, E. Bruendermann, A.-S. Mueller,
Karlsruhe Institute of Technology, Karlsruhe, Germany

Abstract

The linac-based test facility FLUTE (Ferninfrarot Linac-Und Test-Experiment) at the Karlsruhe Institute of Technology (KIT) was designed as a test bench for accelerator technologies with a broad range of beam parameters. The electron bunches are generated in a UV photo-injector, which offers laser pulse shaping as control of the beam parameters. The imprint of a transverse laser profile modulated by a spatial light modulator (SLM) onto the electron bunch was demonstrated at the low energy section of FLUTE. The addition of the linear acceleration structure and bunch compressor section, as well as the upgrade of the RF system, enables experiments with short-pulse electron bunches up to 90 MeV. For this contribution, the SLM was used to recreate the modified electron bunch profile and we present the observed characteristics after passing the traveling-wave RF structure and magnetic chicane.

INTRODUCTION

The electron bunch parameters at modern accelerators are aimed at low emittance and high brightness. In a photo-injector configuration, laser pulse shaping in longitudinal and transverse directions enables direct control over the electron bunch [1]. Combined with machine learning algorithms [2], the laser pulse parameters can be adjusted and long-term effects compensated. Studies indicate that homogeneous ellipsoidal profiles can mitigate space charge effects more effectively than Gaussians [3]. Furthermore, adaptable laser pulse shaping could open the possibility for novel diagnostic approaches with spatial and temporal designs.

In a pixel-based modulation, a liquid crystals SLM allows the influence of intensity and/or phase of the incident laser pulses [4]. The phase of the incident light passing through the liquid crystal pixels is affected, depending on the electrode settings. Each pixel can be modulated independently, resulting in a modulation of the whole laser pulse on the sensor. To generate images in the transverse distribution of the laser pulse, a phase mask known as computer generated hologram (CGH) has to be loaded onto the SLM. An algorithm using inverse Fourier transforms, the Grechberg-Saxton (GS) algorithm can be used for the calculation of the CGH. Spatial light modulators (SLMs) have been used, for instance, at Cornell University [5], DESY [1, 6], and the Daresbury Laboratory [7] to optimize beam homogeneity and reduce emittance.

The modulation of the photo-injector was demonstrated at FLUTE in [8] and [2] where two separated electron bunches were generated simultaneously with the modulated laser pulse. These electron bunches were investigated in the low energy section including one RF structure. Since the first SLM operation at FLUTE, the traveling wave linac and bunch compressor have been added. Furthermore, the laser system was exchanged with a new version, slightly increasing the maximum uncompressed pulse energy to 9 mJ.

* thiemo.schmelzer@kit.edu

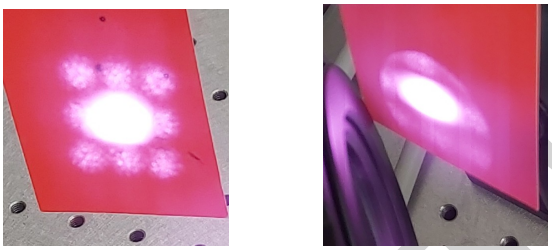

(a) Laser pulse with 3x3 grid modulation 2 m after SLM.

(b) Modulated spots clipping at mirror aperture after 4 m.

Figure 1: Effect of divergence on the spatially modulated laser pulse after the SLM. The high intensity of the non-modulated zero-order is not yet removed.

EXPERIMENTAL SETUP

The experiments were performed at the fully operational test facility FLUTE, where the SLM setup was implemented as selectable addition to the laser pulse transport system. The added flip mirrors allow for simple and reproducible comparison of the laser path with and without the spatial light modulation active.

Transverse Laser Pulse Shaping

At FLUTE the uncompressed laser pulse is transported towards the photo-injector. Next to the start of the accelerator, an optical table for pulse selection, pulse compression and UV-conversion, and a dispersive pulse stretcher is installed. The liquid crystal SLM used for the presented experiments was a commercially available Hamamatsu LCoS-SLM [9], which is optimized for a wavelength range of 800 nm ± 50 nm. In these experiments, the aim was to modulate the transverse laser pulse profile. Therefore, the SLM was installed with a flip mirror setup as a side arm to the main laser path. During installation, it was noticed that the laser beam divergence after the SLM was significantly higher than at normal operation. This led to clipping at the optical components next to the photo-injector. A 1:1 telescope was installed after the SLM, to compensate for the divergence so later optical components could be used without adjustment.

The laser transport from SLM to the optical table next to the photo-injector consists of 2” dielectric mirrors. Especially for holographic images, the divergence of the modu-

lated laser was too high and led to clipping inside the laser transport as shown in Fig. 1. As modulation, a 3x3 grid of small dots was used as reference image. The higher intensity in the center comes from the non-modulated zero-order.

The effective aperture of the optical components on the optical table, e.g., UV-conversion and pulse stretcher, limited the available size of the modulation further. For the experiments, a blazed grating modulation was used as shown in Fig. 2, generating a line of transversely separated dots.

As first component on the optical table, a polarization-based pulse picker is installed to reduce the laser repetition rate to match the RF system. The non-modulated zero-order was passing the optical component, however, the modulated parts were stopped. Rotating the laser polarization by 90° after the SLM resolved this issue and removed the zero-order from the modulated laser pulse.

Accelerator Settings and Diagnostics

During the SLM experiments, the two klystrons powering the photo-injector and the linac were operated at 10 Hz repetition rate. The beam energy after the electron gun was ≈ 5 MeV and ≈ 30 MeV after the linac.

The laser pulse was monitored on a virtual cathode simultaneously to the electron diagnostics. The virtual cathode is a YAG:CE screen positioned at the same distance from a beam splitter as the photocathode and monitored by a camera.

The electron bunches could be detected with multiple profile monitors along the accelerator. The monitors consist of insertable YAG fluorescence screens monitored by high resolution cameras [10]. The first monitor is installed at the end of the low-energy section before the linac. After the linac, a total of four screens are available, two after the linac, one screen at the dispersive section in the center of the magnetic chicane and one close to the end of FLUTE.

RESULTS

The modulated laser pulse was used to generate two spatially separated electron bunches at the FLUTE photo-injector system, thus recreating previous results, now with the updated laser system. Furthermore, the two co-propagating bunchlets were injected into the RF linac and accelerated up to ≈30 MeV. It could be shown, that the separation is preserved and even more prominent at the higher energy, as visible in Fig. 2. In the center (1) the transverse electron bunch profile as observed in the low-energy section is shown. The two bunchlets are very close to each other, where the one to the right has a higher charge than the left bunchlet. This matches with the intensity profile of the laser pulse taken at the virtual cathode. In the lower image (2) the electron bunch profile is shown as observed directly after the linac. The separation of the two bunches increased after the acceleration. These measurements show, that a modulated laser profile can be used to imprint structures on the electron bunch and keep these structures even after additional acceleration.

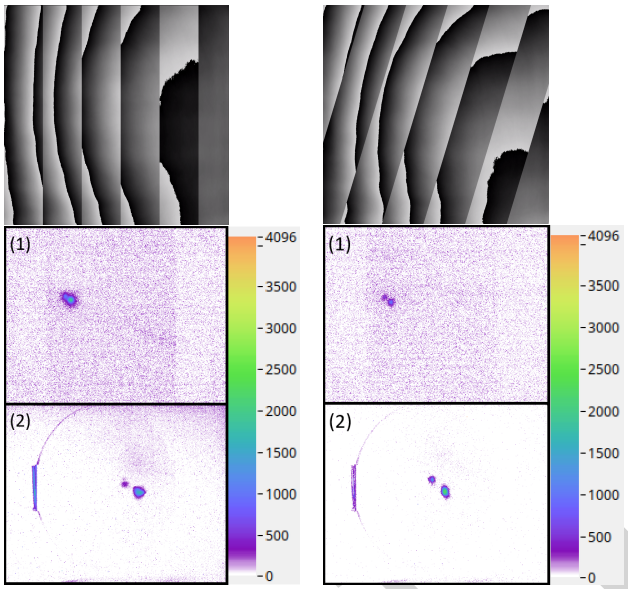

(a) grating rotation 0° (b) grating rotation 20°

Figure 2: Rotated electron bunchlets by angled grating. For both rotations, the upper row shows the CGH applied to the SLM for the blazed gratings. In the middle row (1) a recording of the YAG screen in the low energy section is displayed and in the lower row (2) the image of the same bunchlets at the YAG screen after the linac are shown.

Blazed Grating Rotation

The long laser propagation path after the SLM prohibited the imprinting of complex structures onto the electron bunch as well as freely changing the bunch position by adjusting the holographic image. However, it was possible to rotate the blazed grating and in result rotate the line of diffracted laser dots. This rotation is shown in Fig. 2 as a comparison to the non-rotated grating. The top image shows the calculated CGH at 0° (a) and 20° (b) rotation. The calculation includes a compensation lens for the SLM surface curvature. Comparing the relative bunch position after the linac (2) shows a clockwise rotation from (a) to (b) fitting to about 20°. Unfortunately, the reduced aperture along the laser path led to the need for re-adjustment of the path after each change at the SLM, in order to get two or more of the diffracted laser spots onto the cathode.

Quadrupole Focusing

To test the possibility of steering and controlling the two co-propagating bunchlets, the quadrupole triplet after the linac was used. It is usually used to focus the electron bunch before entering the bunch compressor. The effect of the triplet on the two bunchlets is shown in Fig. 3 at three different focusing strengths, where in (a) the strongest settings were used and in (c) the weakest settings. The symmetric transverse movement from (c) to (a) shows a common focus point, indicating the same central electron energy for the two bunches and a symmetric position around the ideal beam path through the center of the quadrupole.

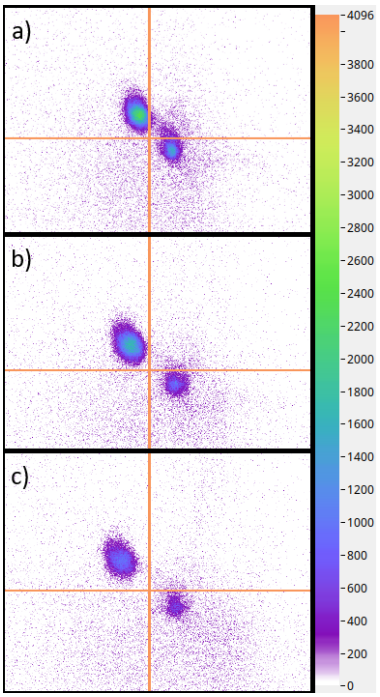

Figure 3: The effect of quadrupole focusing of the modulated bunch consisting of two bunchlets is shown for three different focusing strength from strong in a) to weak in c).

Dispersive Section

After the linear accelerator, the bunch compressor is available and provides a dispersive section with a profile monitor in the middle of the magnetic chicane. Besides the main functionality as bunch compressor, this dispersive section can be employed for studying the beam energy and energy spread. The two bunchlets are shown for two different settings of the chicane in Fig. 4. The left plot (Fig. 4a) shows the bunchlets with the chicane set at a small angle of 5°. The dispersion is low and the horizontal size of the bunchlets is only slightly increased. The second example, was recorded with the chicane set to 14°. The increase in dispersion leads to a significant horizontal widening (Fig. 4b). The increase in size is very similar for both bunchlets. This demonstrates that their energy spread is close to equal. Furthermore, although the two spots have a small horizontal separation, it remains the same for the different amounts of dispersion, indicating the two bunchlets have the same energy. This indicates that the two bunchlets were truly generated by two purely spatially separated laser spots, without a significant temporal offset. As such an offset would lead to the two bunchlets experiencing different acceleration phases in the linac and gaining a different energy as well as energy spread.

SUMMARY AND OUTLOOK

With a spatial light modulator in the laser path to the photo-injector, a transverse modulation resulting in the generation of two spatially separated electron bunchlets was demonstrated. We could show that the separation was preserved throughout the whole accelerator. The existing diagnostics

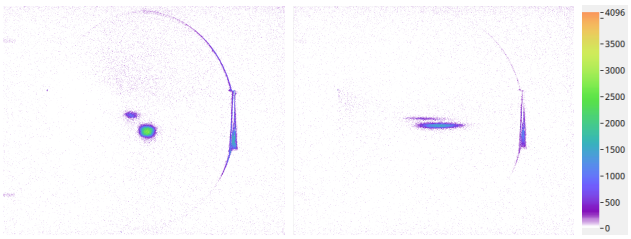

(a) Chicane at 5° (b) Chicane at 14°

Figure 4: Modulated electron bunch in dispersive section. The difference in the horizontal size between the low dispersion setting (a) and the high dispersion setting (b) shows the contribution by the energy spread to be the same for both bunchlets.

allowed detailed monitoring of the spatial distribution along the path, from the laser distribution on the cathode to the electron distribution at different positions in the accelerator. The relative orientation of the bunchlets to each other could be influenced by rotating the modulated blazed grating. The non-modulated zero-order contribution in the resulting laser spot could be removed by rotating the laser polarization after the SLM and before a polarization sensitive filter. Using quadrupole magnets, it was possible to control the position of the bunchlets. With the dispersive section in the bunch compressor, we demonstrated that the bunchlets have the same energy and energy spread and purely differ in their transverse position.

Next steps will include the redesign of the SLM setup, with the option to place the setup closer to the photo-injector, directly before the third harmonic generation (THG) stage converting the infrared (800 nm) laser to UV (266 nm). This would reduce the optical path after modulation by over 20 meters and improve the laser modulation capabilities on the photocathode.

REFERENCES

[1] D. Ilia *et al.*, "Novel photoinjector laser providing advanced pulse shaping for FLASH and EuXFEL", in *Proc. IPAC'25*, Taipei, Taiwan, Jun. 2025, pp. 2564–2567. doi:10.18429/JACoW-IPAC2025-THPB027

[2] C. Xu, "Automatic Control of Linear Particle Accelerators with Machine Learning Methods", Dissertation, Fakultät für Physik, Karlsruher Institut für Technologie, Karlsruhe, Germany, 2025. doi:10.5445/IR/1000178623

[3] O. J. Luiten, S. B. Van Der Geer, M. J. De Loos, F. B. Kiewiet, and M. J. van der Wiel "How to Realize Uniform Three-Dimensional Ellipsoidal Electron Bunches", Phys. Rev. Lett., vol. 93, no. 9, p. 094802, Aug. 2004. doi:10.1103/PhysRevLett.93.094802

[4] Carmelo Rosales-Guzmán and Andrew Forbes, *How to Shape Light with Spatial Light Modulators*, Bellingham: Society of Photo-Optical Instrumentation Engineers SPIE, 2017. doi:10.1117/3.2281295

[5] J. Maxson, H. Lee, A. C. Bartnik, J. Kiefer and I. Bazarov, "Adaptive Electron Beam Shaping Using a Photoemission Gun and Spatial Light Modulator", *Phys. Rev. Spec. Top.*

Accel. Beams, vol. 18, no. 2, p. 023401, Feb. 2015. doi:10.1103/PhysRevSTAB.18.023401

[6] C. Koschitzki, *et al.*, "Chirped pulse laser shaping for high brightness photoinjectors", in *Proc. FEL'22*, Trieste, Italy, Aug. 2022, pp. 345–348. doi:10.18429/JACoW-FEL2022-WEAO4

[7] A. E. Pollard, D. J. Dunning, W. A. Okell, and E. W. Snedden, "Machine Learning Approach to Temporal Pulse Shaping for the Photoinjector Laser at CLARA", in *Proc. IPAC'22*, Bangkok, Thailand, Jun. 2022, pp. 2917–2920. doi:10.18429/JACoW-IPAC2022-THPOTK061

[8] M. Nabinger *et al.*, "Transverse and Longitudinal Modulation of Photoinjection Pulses at FLUTE", in *Proc. IPAC'22*, Bangkok, Thailand, Jun. 2022, pp. 1174–1177. doi:10.18429/JACoW-IPAC2022-TUPOPT068

[9] Hamamatsu, LCOS-SLM (Optical phase modulator) X15213-02L, https://www.hamamatsu.com/eu/en/product/optical-components/lcos-slm/high_power_laser_type/X15213-02L.html

[10] M. Yan *et al.*, "FLUTE Diagnostics Integration", in *Proc. IPAC'18*, Vancouver, Canada, Apr.-May 2018, pp. 2227–2229. doi:10.18429/JACoW-IPAC2018-WEPAL029